Molecular and Supramolecular Structural Studies on Human Tropoelastin Sequences

Angela Ostuni, Brigida Bochicchio, Maria F. Armentano, Faustino Bisaccia, and Antonio M. Tamburro
Department of Chemistry, University of Basilicata, Potenza, Italy

ABSTRACT One of the unusual properties of elastin is its ability to coacervate, which has been proposed to play an important role in the alignment of monomeric elastin for cross-linking into the polymeric elastin matrix. The temperature at which this transition takes place depends on several factors including protein concentration, ionic strength, and pH. Previously, polypeptide sequences encoded by different exons of the human tropoelastin gene have been analyzed for their ability to coacervate and to self-assemble. Few of them were indeed able to coacervate and only one, that encoded by exon 30 (EX30), gave amyloid fibers. In this article, we report on two chemically synthesized peptides—a decapeptide and an octadecapeptide—whose sequences are contained in the longer EX30 peptide and on a polypeptide (EX1–7) of 125 amino-acid residues corresponding to the sequence coded by the exons 1–7 and on a polypeptide (EX2–7) of 99 amino-acid residues encoded by exons 2–7 of human tropoelastin obtained by recombinant DNA techniques. Molecular and supramolecular structural characterization of these peptides showed that a minimum sequence of ~20 amino acids is needed to form amyloid fibers in the exon 30-derived peptides. The N-terminal region of mature tropoelastin (EX2–7) gives rise to a coacervate and forms elastinlike fibers, whereas the polypeptide sequence containing the signal peptide (EX1–7) forms mainly amyloid fibers. Circular dichroism spectra show that β-structure is ubiquitous in all the sequences studied, suggesting that the presence of a β-structure is a necessary, although not sufficient, requirement for the appearance of amyloid fibers.

INTRODUCTION

The elastic properties of several vertebrate tissues such as lung, skin, and large blood vessels are mainly due to the presence of elastin in the elastic fibers (1,2). The monomeric form, tropoelastin, is a soluble protein that undergoes cross-linking and assembly into elastic fibers in the extracellular matrix. The details of the events that induce elastic fiber assembly are still unknown at the molecular level. Recently, some studies have shown the importance of self-assembly of tropoelastin for elastic-fiber formation (3). Furthermore, it has been demonstrated that short peptides and recombinantly expressed polypeptides based on sequences of human elastin are able to give filaments with supramolecular organization similar to that found for the entire protein (4,5). One of the unusual properties of elastin is its ability to undergo coacervation, a self-aggregation process in which the protein comes out of solution as a second phase on an increase in temperature. Coacervation, which has been proposed to concentrate and to align tropoelastin molecules for cross-linking, a key step in elastogenesis (6), was first demonstrated with heterogeneous mixtures of polypeptides such as α-elastin and κ-elastin prepared by hydrolytic solubilization of insoluble polymeric elastin (7–10). Subsequently, both synthetic polypeptides corresponding to hydrophobic domains of elastin (4,5,11,12) and full-length tropoelastin (13–15) have also been shown to undergo this process, related to the predominantly nonpolar character of these polypeptides. The temperature at which this transition takes place is dependent on several factors including protein concentration, ionic strength, and pH (15,16). In contrast to heat-induced protein denaturation, which results in disordered molecular structures, coacervation of tropoelastin and elastin polypeptides has been shown to promote the formation of spherical droplets and of well-ordered filamentous structures at least at the supramolecular level (13,14,17–19). For this reason, it has been proposed that coacervation might play an important physiological role in the ordering and alignment of monomeric elastin for cross-linking into the polymeric elastin matrix (14,19,20).

To understand the mechanism of supramolecular assembly of elastin and the relationships between structural organization and physical properties, polypeptide sequences encoded by some exons of the human tropoelastin gene have been analyzed for their ability to coacervate and to self-assemble. The great majority of them were shown to form organized structures, but only a few were indeed able to coacervate and only one, that encoded by exon 30 (EX30), gave an irreversible precipitation (21,22). Interestingly, previous studies have demonstrated that EX30 of human tropoelastin, belonging to the C-terminal region of the protein, gives rise to amyloid fibers depending on microenvironment conditions such as pH, temperature, and peptide concentration (23). Concerning elastin, our group has also studied the elastinlike polymer poly (VGGVG) and has demonstrated that it gives rise to amyloidlike fibers such as EX30. Interestingly, the sequence encoded by EX30 contains the motif XGGZG (X, Z=V, L) found in many proteins such as collagens IV and VII, major prion protein precursor, amyloid βA4 precursor

Submitted April 16, 2007, and accepted for publication June 11, 2007.

Address reprint requests to A. M. Tamburro, Tel.: 39-0-971-202242; E-mail: antonio.tamburro@unibas.it.

Editor: Jane Clarke.

0006-3495/07/11/3640/12 $2.00

doi: 10.1529/biophysj.107.110809

protein-binding family, etc., thus suggesting that this sequence could be involved in contributing to the self-assembly of amyloid fibers even in other proteins. The XGGZG motif is also found in the N-terminal region of human tropoelastin, specifically in the sequence encoded by exon 7 of the gene of human tropoelastin. Furthermore, when the sequence encoded by EX30 is inserted in a longer polypeptide, it does not form amyloidlike fibrils (6). This observation suggests the investigation of the minimum sequence able to give amyloid fibers and of the role of the neighboring sequence.

Accordingly, we have chemically synthesized two peptides, a decapeptide (together with its cyclic counterpart, cyclodecapeptide) and an octadecapeptide, whose sequences are contained in the longer EX30. A peptide (EX1), corresponding to the signal peptide sequence, a polypeptide of 125 amino-acid residues (EX1–7) corresponding to the sequence coded by the exons 1–7, and a polypeptide (EX2–7) of 99 amino-acid residues, encoded by the exons 2–7 of human tropoelastin, were also synthesized (see Table 1) by different techniques (see Materials and Methods). Structural and suprastructural characterization of these peptides showed that a minimum sequence of ~20 amino acids is needed to form amyloid fibers. The N-terminal region of mature tropoelastin gives rise to a coacervate and forms elastinlike fibers, whereas the polypeptide sequence containing the signal peptide forms mainly amyloid fibers.

MATERIALS AND METHODS

Chemical synthesis and purification of peptides—EX1

MAGLTAAAPRPGVLLLLLSILHPSRPG, octadecapeptide LGGLGVGG-LGVPGVGGLG, and decapeptide LGGLGVGGLG were synthesized using standard fluorenyl-methoxy-carbonyl solid phase chemistry on a Pioneer synthesizer (PE Biosystems, Foster City, CA). Coupling reagents (0.5 M PyBop/dimethyl formamide and 1.0 M diisopropylethylamine/dimethyl formamide) were used with a fourfold excess of amino acid. Trifluoroacetic acid (TFA)/H_2O/thioanisole/phenol/ethanedithiol (88%, 3%, 3%, 4%, 2%) mixture was used for the deprotection and cleavage of the peptides (24). Crude peptides were precipitated in cold diethyl ether and then lyophilized. Purification of the peptides was carried out on a reverse-phase C_{18} column (25 × 300 nm, 5 μm particles) using a gradient of acetonitrile/water in 0.1% TFA. Sample identity was confirmed with electrospray mass spectroscopy. The mass data for the synthetic peptides are shown in the Supplementary Material.

To synthesize cyclo-(LGGLGVGGLG), 0.11 mmol of LGGLGVGGLG (1 equivalent) were dissolved in the minimum volume of dimethyl sulfoxide. Then 20 μL of triethylamine (TEA, 2.5 equivalents) were added to the reaction mixture followed by 35.7 μL of diphenyl phosphoryl azide (DPPA; 1.5 equivalents). After stirring the reaction mixture, 19 μL of TEA were added. After 55 h, 35.7 μL of DPPA and 39 μL of TEA were further added. After 45 h, 35.7 μL of DPPA and 39 μL of TEA were newly added. The reaction product was precipitated by addition of diethyl ether. After elimination of supernatant, the oily product obtained was dissolved in a mixture of acetonitrile/water and lyophilized. The obtained compound was an oil that was solubilized in a minimum volume of ethyl alcohol and then precipitated in diethyl ether, giving rise to a solid powder after 48 h at 4°C.

TABLE 1 The human tropoelastin sequence

	EX1		|EX2		|EX3	|EX4
1	MAGLTAAAPR	PGVLLLLLSI	LHPSRPGGVP	GAIPGGVPGG	VFYPGAGLGA	LGGGALGPGG
	|**EX5**	|**EX6**			|**EX7**	
61	***KPLKPVPGGL***	***AGAGLGAGLG***	***AFPAVTFPGA***	***LVPGGVADAA***	***AAYKAAKAGA***	***GLGGVPGVGG***
	|**EX8**		|**EX9**	|**EX10**		
121	***LGVSA***GAVVP	QPGAGVKPGK	VPGVGLPGVY	PGGVLPGARF	PGVGVLPGVP	TGAGVKPKAP
	|**EX11**	|**EX12**		|**EX13**	|**EX14**	
181	GVGGAFAGIP	GVGPFGGPQP	GVPLGYPIKA	PKLPGGYGLP	YTTGKLPYGY	GPGGVAGAAG
	|**EX15**		|**EX16**		|**EX17**	
241	KAGYPTGTGV	GPQAAAAAAA	KAAAKFGAGA	AGVLPGVGGA	GVPGVPGAIP	GIGGIAGVGT
		|**EX18**				
301	PAAAAAAAAA	AKAAKYGAAA	GLVPGGPGFG	PGVVGVPGAG	VPGVGVPGAG	IPVVPGAGIP
	|**EX19**		|**EX20**			
361	GAAVPGVVSP	EAAAKAAAKA	AKYGARPGVG	VGGIPTYGVG	AGGFPGFGVG	VGGIPGVAGV
		|**EX21**		|**EX22**		
421	PSVGGVPGVG	GVPGVGISPE	AQAAAAAKAA	KYGAAGAGVL	GGLVPGPQAA	VPGVPGTGGV
	|**EX23**		|**EX24**			
481	PGVGTPAAAA	AKAAAKAAQF	ALLNLAGLVP	GVGVAPGVGV	APGVGVAPGV	GLAPGVGVAP
		|**EX25**		|**EX26**		
541	GVGVAPGVGV	APGIGPGGVA	AAAKSAAKVA	AKAQLRAAAG	LGAGIPGLGV	GVGVPGLGVG
		|**EX26A**		|**EX27**		
601	AGVPGLGVGA	GVPGFGAGAD	EGVRRSLSPE	LREGDPSSSQ	HLPSTPSSPR	VPGALAAAKA
	|**EX28**		|**EX29**		|**EX30**	
661	AKYGAAVPGV	LGGLGALGGV	GIPGGVVGAG	PAAAAAAAKA	AAKAAQF***GLV***	***GAAGLGGLGV***
		|**EX31**	|**EX32**		|**EX33**	|**EX36**
721	***GGLGVPGVGG***	***LG***GIPPAAAA	KAAKYGAAGL	GGVLGGAGQF	PLGGVAARPG	FGLSPIFPGG
781	ACLGKACGRK	RK				

The peptide sequences studied are underlined and in italics. The exon boundaries are also indicated.

PCR amplification of human elastin CDNA

The region of DNA corresponding to the first seven exons of the human tropoelastin (coding for 125 amino acids included the signal peptide) was amplified from the human lung cDNA (BD Biosciences Clontech. Mountain View, CA) by polymerase chain reaction (PCR), using specific primers. The forward primer 5′-TCGC[GGATCC]ATGGCGGGTCTGACGGCG-3′ and the reverse primer 5′-CGAGGTACC[GAATTC]TCATGCAGACACTCC-TAAGC-3′ were designed to introduce *Bam*HI and *Eco*RI restriction sites into the PCR product for efficient cloning purpose into a cloning vector pGEX-2T (Amersham, Piscataway, NJ). Amplification was carried out in a 25-μl reaction volume containing 0.5 ng of template, 0.4 μM of each primer, 0.4 mM dNTPs, 2.5 mM $MgCl_2$, 2.5 units of Taq polymerase (Euroclone, Celbio, Milan, Italy), and PCR buffer supplied with the enzyme. PCR reaction was carried out on a PCR system (Thermo Hybaid, Ulm, Germany). PCR mixture was initially denatured at 95°C for 2 min followed by amplification using 30 cycles of denaturation (45 s at 94°C), annealing (55°C for 1 min), and extension (2 min at 72°C) with the final extension lasting 5 min. The PCR product was revealed on a 1% agarose gel, and the band corresponding to the desired PCR product was purified from the gel using a Gel Extraction kit (GenoMed, St. Louis, MO).

Construction of expression vector

The elastin polypeptide construct was designed as glutathione S-transferase (GST) fusion protein. Tropoelastin fragment (EX1–7) and the pGEX-2T vector were digested with the enzymes, *Bam*HI and *Eco*RI, and ligated. After ligation, TG1 cells (Stratagene, La Jolla, CA) were transformed with the recombinant vector (recombinant vector I). The sequence and the correct orientation of the insert were confirmed by DNA sequencing (MWG-Biotech, Ebersberg, Germany). Moreover, by means of a QuikChange Site-Directed Mutagenesis Kit (Stratagene) we have mutated the 77C of the CTG codon into an ATG codon changing the proline 26 to methionine (recombinant vector II).

Expression and purification of elastin polypeptides

The recombinant vectors (I and II) were used to transform Rosetta pLys(S) cells (Stratagene) for expression of the polypeptides. A single colony was used to inoculate, overnight at 37°C with shaking, 2 ml Luria broth containing 100 μg/ml ampicillin and 34 μg/ml chloramphenicol. The culture was diluted 1:50 and the expression of the GST fusion proteins was induced at the exponential phase of growth by the addition of isopropyl-thiogalactoside to a final concentration of 0.1 mM in the culture. The cells were collected by centrifugation 5 h after induction and suspended in 2 ml of Tris 10 mM, EDTA 1 mM, pH 7 (TE buffer). After sonication, cells were recovered by centrifugation and were resuspended in 1 ml of TE buffer. Proteins were analyzed by SDS-PAGE, and after electroblotting, the nitrocellulose sheets were treated with polyclonal antiserum to human tropoelastin (Elastin Products, Owensville, MO), and then incubated with horseradish peroxidase-conjugated anti-rabbit IgG. The immunoreaction was detected by the peroxidase reaction performed with 20 μm of a mixture of 4-chloro-1-naphthol (0.05% w/v), methanol (16% v/v), and bovine serum albumin (0.5% w/v) in a medium containing 0.14 M phosphate (pH 7.0) with the final addition of 10 μL of 30% H_2O_2 (see Supplementary Material). EX1–7 and EX2–7 were cleaved from the GST fusion protein using cyanogen bromide 80 μM in 70% formic acid at room temperature for 6 h. Solution containing cleavage products was then diluted 1:10 with distilled water and was left uncovered overnight in the fume hood to remove residual cyanide vapor; finally it was frozen, and lyophilized. The elastin polypeptides were purified on a reverse-phase C_{18} column (25 × 300 nm, 5 μm particles) using a gradient of acetonitrile/water in 0.1% TFA. The purity of polypeptides was assessed by electrospray mass spectroscopy.

Circular dichroism

Circular dichroism (CD) spectra were recorded on a JASCO 600A automatic circular dichrograph equipped with a thermoelectric temperature controller, using a 0.1-cm cylindrical quartz cell with samples at the indicated concentrations and temperatures (JASCO, Tokyo, Japan). Spectra were obtained with 0.1 nm steps from 190 to 250 nm, 1 nm bandwidth, a time constant of 0.5 s and 20 mdeg of sensitivity. After the baseline spectra of the solvents were subtracted, spectra were smoothed using the Fourier transform routine of the J-600A. Data were expressed in terms of the molar ellipticity per residues $[\theta]_{MRW}$ and the molar ellipticity $[\theta]_M$ in units of deg cm^2 $dmol^{-1}$. Analysis of the CD spectra for determining the secondary structure was performed with the CONTIN program (CDPro software package available at http://lamar.colostate.edu/~sreeram/CDPro/main.html).

Turbidimetry measurements

These measurements were performed using a spectrophotometer Varian Cary 3 equipped with a temperature controller (Varian, Palo Alto, CA). Polypeptide at the indicated concentration was dissolved in water, and in phosphate-buffered saline (PBS) (141 mM NaCl, 2.7 mM KCl, 10 mM Na_2HPO_4, and 1.5 mM KH_2PO_4). Solutions were placed in a quartz cuvette and allowed to equilibrate for 5 min in the sample cell of the spectrophotometer. Then the temperature was increased at a rate of 2°C/min with stirring. Turbidity on apparent absorbance TAA was monitored at 440 nm.

Transmission electron microscopy

Polypeptide was dissolved either in water or in PBS at the indicated concentration and incubated at 60°C for the indicated time. Specimens were prepared by putting a carbon-coated grid on a drop of sample for 1 min. The grid was rinsed with 20 drops of water and then stained with 10 drops of a 2% uranyl acetate solution (pH 3.5). Specimens were examined on a Zeiss EM 10 electron microscope at an accelerating voltage of 60 kV (Carl Zeiss, Jena, Germany).

Atomic force microscopy

The structural study has been carried out by use of Multimode NanoScope IIIa (Digital Instruments, Santa Barbara, CA) using silicon substrates. All experimental data were collected in tapping mode, using scanner J (scan range 100 μm) and standard Si probes (NT-MDT, Zelenograd, Russia). Scan rates were ~1 Hz.

Light microscopy

Images were acquired with a Leica MZ15 microscope, equipped with a DC500 digital camera (Leica, Wetzlar, Germany).

Congo red birefringence assay

Ten microliters of EX1–7 (250 μM in water) were incubated at 60°C for two days and air-dried on a glass microscope slide. The staining working solution was prepared by adding a saturating amount of Congo Red in 80% ethanol, 20% water, and saturating amount of NaCl. After filtration, 50 μl of staining solution were placed onto the dried polypeptide sample, the excess of solution was removed, and the stained sample was examined under polarized light with a Nikon ECLIPSE E600 POL microscope equipped with Nikon Cool Pix 4500 4.0 Mega Pixel (Nikon, Tokyo, Japan).

RESULTS

In Fig. 1 *A* are reported the CD spectra of the decapeptide LGGLGVGGLG at different temperatures in PBS. In the

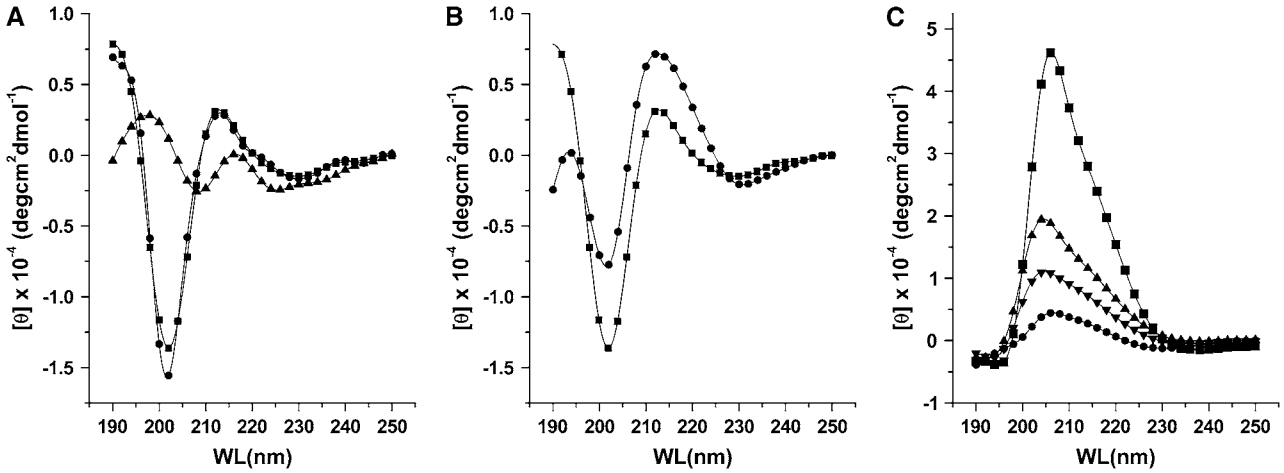

FIGURE 1 CD spectra of the decapeptide 0.1 mg/ml in PBS (*A*) at different temperatures (●) 25°C, (■) 45°C, and (▲) 65°C; (*B*) at 25°C at 0.1 mg/ml (■) and 5 mg/ml (●); (*C*) CD spectra of cyclic decapeptide in water 6 mg/ml and 0°C (■); 0.6 mg/ml and 0°C (▲); 0.6 mg/ml and 25°C (▼); and 0.6 mg/ml and 60°C (●).

range 25–45°C the spectra are interpretable in terms of dominant poly-L-proline II left-handed helix (PPII), as suggested by the small positive band at ~215 nm and by the strong negative band at shorter wavelengths. However, at 65°C the shorter wavelength negative band is replaced by a positive one, as also expected for the coexistence of a type II β-turn. This is further confirmed by the CD spectra reported in Fig. 1 *B*, which were registered for a sample concentration 50-fold higher. Here, the trend on increasing the concentration is that of a trend toward positive values of ellipticity, compatible with an increase of the β-turn contribution. The final confirmation comes from the spectra of the conformationally restrained cyclo-decapeptide showing CD diagnostic of type II β-turn (25). As expected, the β-turn increases on increasing the concentration and on decreasing the temperature (Fig. 1 *C*).

In Fig. 2 *A*, we report the CD difference spectra of the octadecapeptide LGGLGVGGLGVPGVGGLG as a function of temperature in PBS with 200 mM NaCl. The β-sheet contribution to the conformer population is dominant at high temperatures, as evidenced by the strong negative band at ~216 nm and by a positive band at ~200 nm. Fig. 2 *B* shows the CD spectra of the octadecapeptide in water as a function of temperature. The spectrum at 0°C shows a strong negative band at ~200 nm and a trend toward a positive band at 215 nm, both bands being typical of PPII conformation. These conformational features indicate the presence of PPII structure, although together with other conformations present in minor amounts. The increase of the temperature to 25°C, 37°C, and 70°C induces the decrease in intensity and the red shift of the strong negative band and the loss of the positive band at 215 nm. This behavior suggests that, on increasing the temperature, a conformational transition occurs from extended conformations such as PPII, more stable at low temperatures, toward more folded ones such as β-turns and/or to other extended ones such as β-sheet.

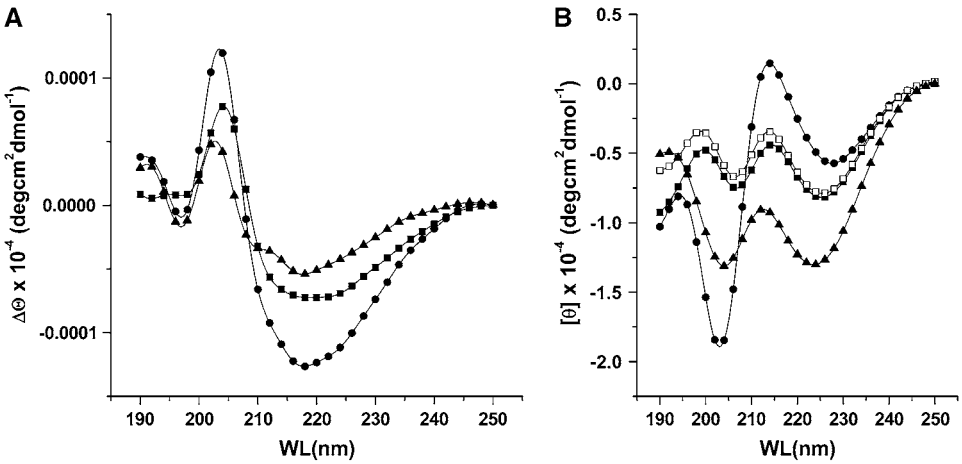

FIGURE 2 (*A*) CD difference spectra of the octadecapeptide 0.7 mg/ml in PBS with NaCl 200 mM 70–25°C (■), 25–0°C (▲), and 70–0°C (●); and (*B*) CD of the octadecapeptide 0.7 mg/ml in water at different temperatures, 0°C (●), 25°C (■), 37°C (□), and 70°C (▲).

Fig. 3 shows the CD spectra of the octadecapeptide in aqueous solution at four different temperatures and at different ionic strengths. At 0°C the CD spectra show the prominent negative band at ~205 nm and a trend toward a positive band at 215 nm, again both bands being typical of the PPII conformation (Fig. 3 *A*). The increase of the ionic strength induces the decrease of the negative band and the near disappearance of that at 215 nm, thus suggesting the destabilization of PPII structure. The CD spectra in aqueous solution at 25°C, 37°C, and 70°C are dominated by negative bands at 205 and 225 nm, whereas the positive band present at 0°C is no longer present. As a whole, the spectra, either as a function of temperature or of ionic strength, indicate the presence of different conformer populations, interchanging among themselves, such as PPII, β-sheet, β-turns, and the so-called unordered forms. At supramolecular level, as reported in Fig. 4 *A*, the transmission electron microscopy (TEM) of the decapeptide shows the twisted-rope motif found in elastin and tropoelastin (14,26). A similar ultrastructural organization is also shown by the octadecapeptide as reported in Fig. 4 *B*, although together with the supramolecular structure shown in Fig. 4, *C* and *D*. Interestingly, the octadecapeptide shows an elastinlike ultrastructure similar to those previously described for the coacervates of tropoelastin and α-elastin (27). In fact, turbidimetry showed for this peptide a coacervation curve, although at very high concentration (15 mM) (data not shown). As expected for a true coacervation, the process was fully reversible. Of particular interest is the beaded-necklace structure, best resolved in Fig. 4 *D*, which is classical for elastin and its derivatives. Again, analogously to elastin, this pattern repeats itself at higher scales on hydrated samples as seen by atomic force microscopy (AFM) (Fig. 5, *A* and *B*). This finding is a strong indication of fractal aspects (28).

Fig. 6 shows the CD spectra of EX2–7 under different conditions. The curves and the related inset indicate a conformational transition essentially from the β-strand in water to α-helix in aqueous 2,2,2-trifluoroethanol (TFE), plus a minor contribution from random coil to α-helix. Furthermore, the

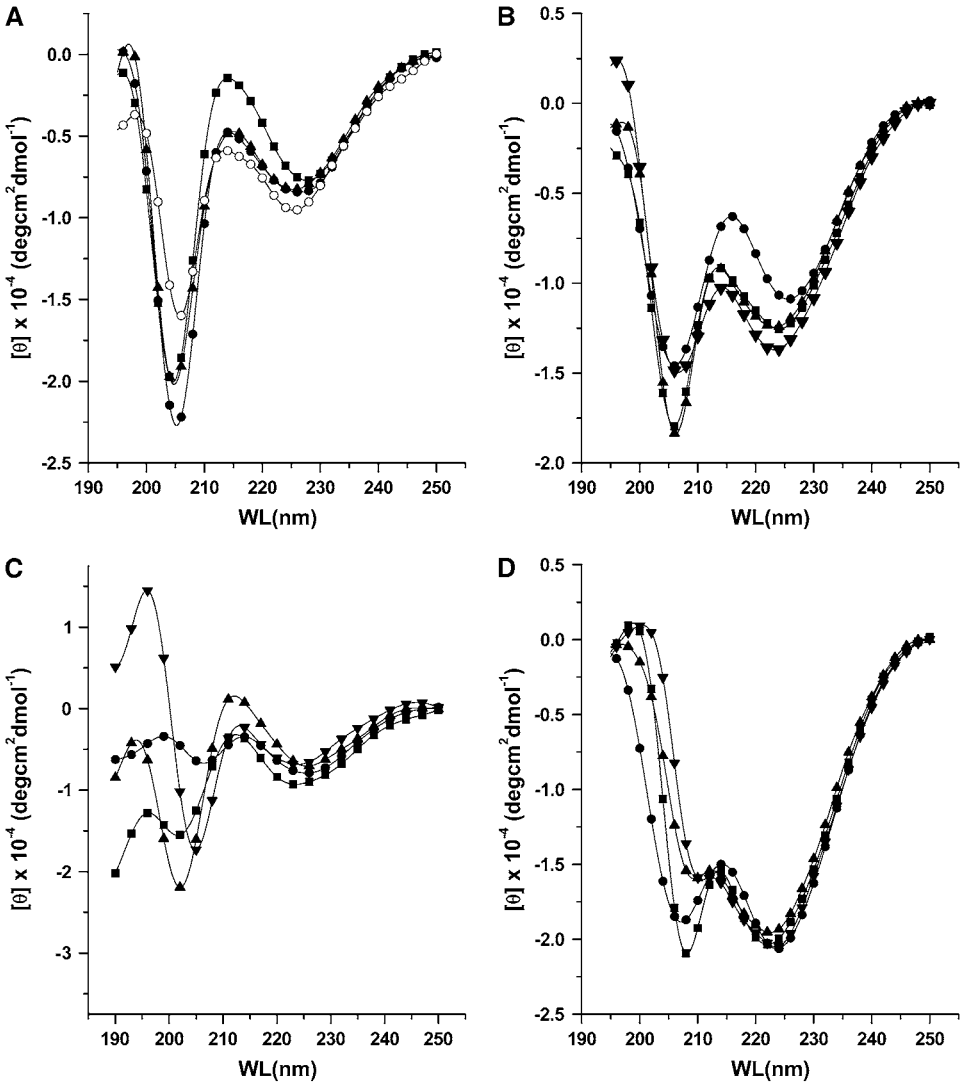

FIGURE 3 CD spectra of the octadecapeptide (*A*) at 0°C in water (●), PBS with 50 mM NaCl (■), PBS with 200 mM NaCl (▲), PBS with 1 M NaCl (○); (*B*) at 25°C in water (●), PBS with 50 mM NaCl (■), PBS with 200 mM NaCl (▲), PBS with 1 M NaCl (▼); (*C*) at 37°C in PBS with 50 mM NaCl (■), PBS with 200 mM NaCl (▲), PBS with 1 M NaCl (▼); and (*D*) at 70°C in water (●), PBS with 50 mM NaCl (■), PBS with 200 mM NaCl (▲), and PBS with 1 M NaCl (▼).

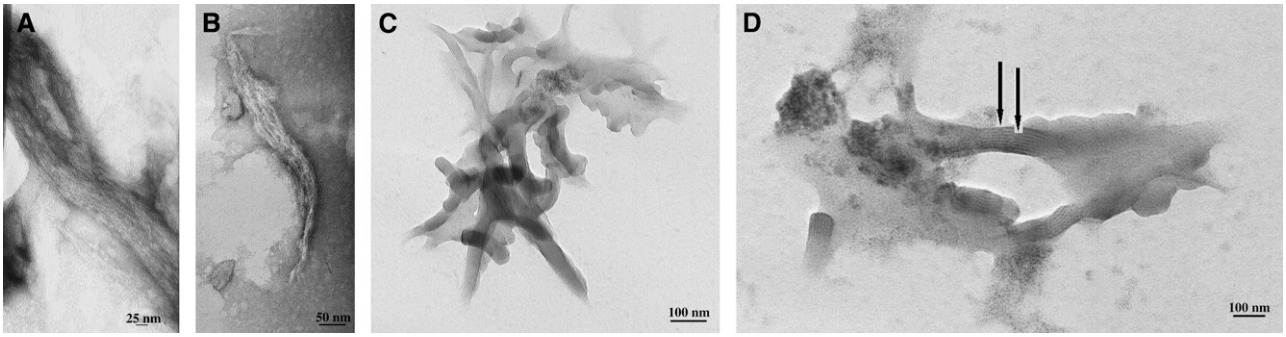

FIGURE 4 TEM micrographs. (*A*) The decapeptide forms twisted-rope filaments. Bar indicates 25 nm. (*B*) The octadecapeptide forms twisted-rope filaments. Bar indicates 50 nm. (*C*, *D*) The octadecapeptide filaments form parallel arrays. In panel *D*, a beaded-necklace structure is appearing and is indicated by the arrows. Bar indicates 100 nm.

polypeptide exhibits at 24 μM and 2X-PBS a process not fully reversible (cooling curve characterized by some extent of hysteresis), therefore suggesting the formation of supramolecular aggregates other than the conventional coacervate (see Supplementary Material). TEM micrographies of this polypeptide show single ribbonlike fibers (Fig. 7 *A*) similar to those found for the peptide PGGLAGAGLGA coded by the exon 5 alone (3) and where the polypeptide chains are in the PPII conformation possibly comprising β-turns. Globules (Fig. 7 *B*) and long unbranched fibrils, tentatively described as amyloidlike on a morphological basis (29), were also observed (Fig. 7 *C*). The same supramolecular structures (twisted ribbons, globules and, possibly, amyloids) are seen at higher scales by AFM on hydrated samples (Fig. 8, *A* and *B*). Optical microscopy showed branched, arborescent amyloid fibers (Fig. 9 *A*). The same fibers in presence of water are shown in Fig. 9 *B*.

CD spectra of EX1–7 under different conditions are reported in Fig. 10. In aqueous solution the curves are very similar to those displayed by tropoelastin (15) and solubilized elastin such as α-elastin (30) and κ-elastin (31). The

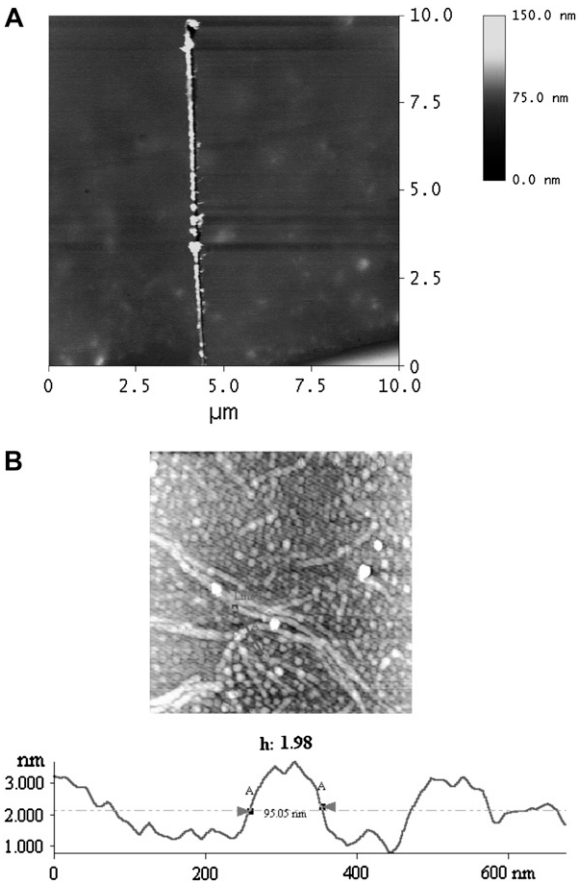

FIGURE 5 AFM micrographs of the octadecapeptide. A beaded-necklace structure is observed (*A*) at measured diameter of a fiber; and (*B*) at ~95 nm (see the *green line* in *image*).

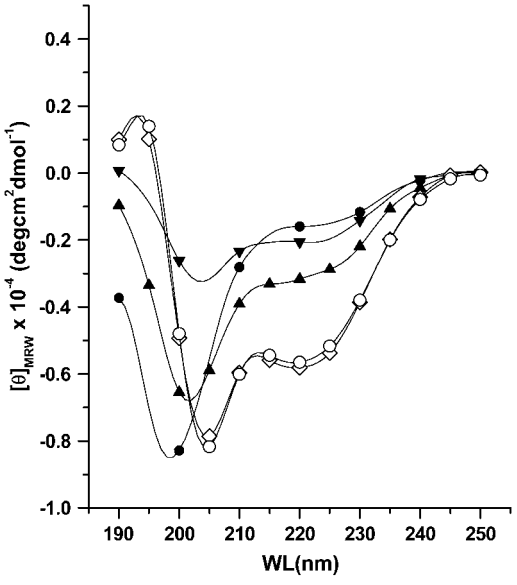

FIGURE 6 CD spectra of EX2–7, 10 μM, and at 25°C in water (●), 10%TFE (▲), 20%TFE (▼), 80% TFE (◇), and 95% TFE (○). The inset shows the fractions of secondary structure estimated from the deconvoluted CD spectra by the Contin method.

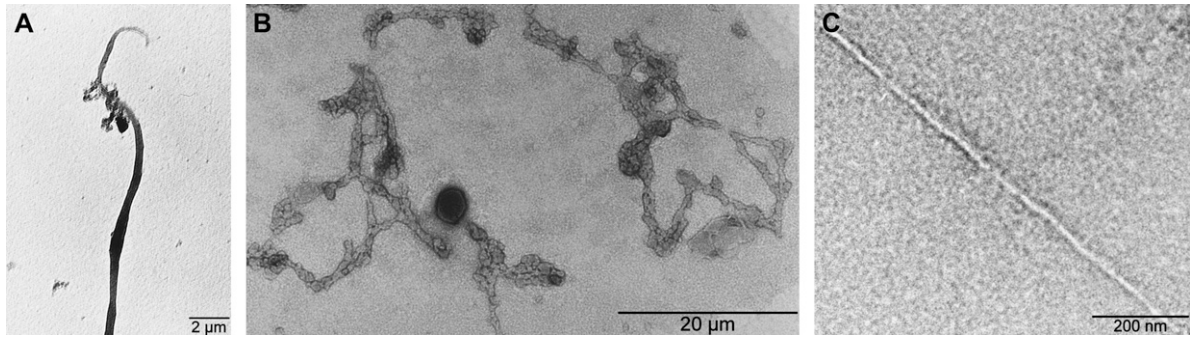

FIGURE 7 TEM micrographs of EX2–7, (*A*) 24 μM in 2X-PBS at 60°C for four days; and (*B* and *C*) 269 μM in water at 60°C for one day.

same is true in aqueous TFE when the organic solvent is at a percentage >20%. Also the secondary structure assignments (see *inset*) are compatible with what is known for tropoelastin, provided it is considered that the algorithm used does not take into account the PPII structure which is rather ubiquitous in tropoelastin (32). It is to be noted that the amount of β-strand reaches the maximum either in aqueous solutions or in 10–20% TFE, whereas, at increasing percentages of TFE, the β-strand is substituted for by the α-helix. Heating induced the aqueous solution to adopt a β-structured state (Fig. 11). This has a counterpart in the behavior of the sequence coded by exon 30 of human tropoelastin (23) (see Discussion). The self-assembly properties of this polypeptide were investigated by turbidimetry as a function of temperature either in water or in PBS (see

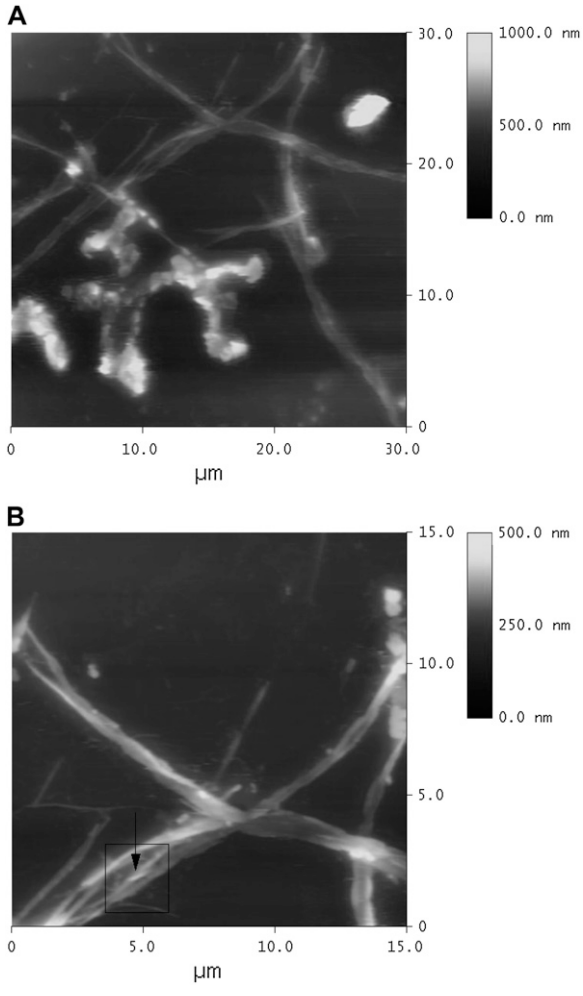

FIGURE 8 AFM micrographs of EX2–7. Globules, ribbon fibers and, possibly, amyloids are observable (*A*). The arrow in the box (*B*) indicates interwound amyloidlike fiber.

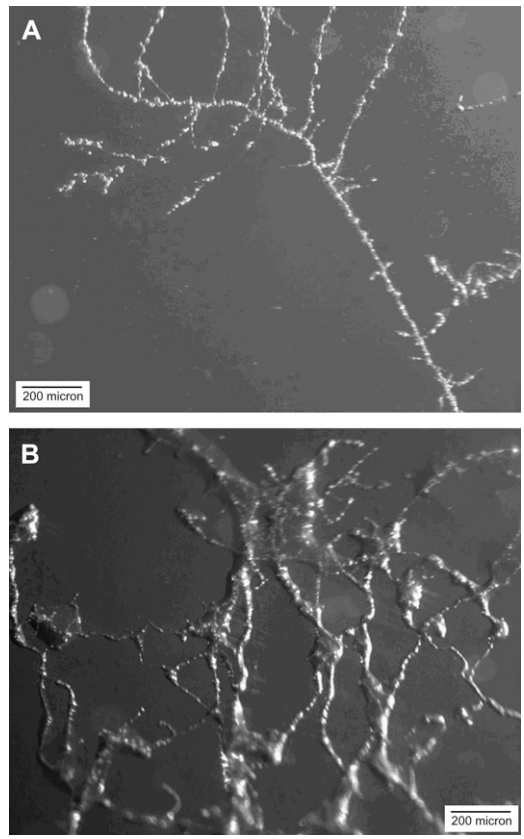

FIGURE 9 Optical microscopy images. (*A*) EX2–7 forms branched, arborescent amyloid fibers; and (*B*) EX2–7 with water. Bar indicates 200 μm.

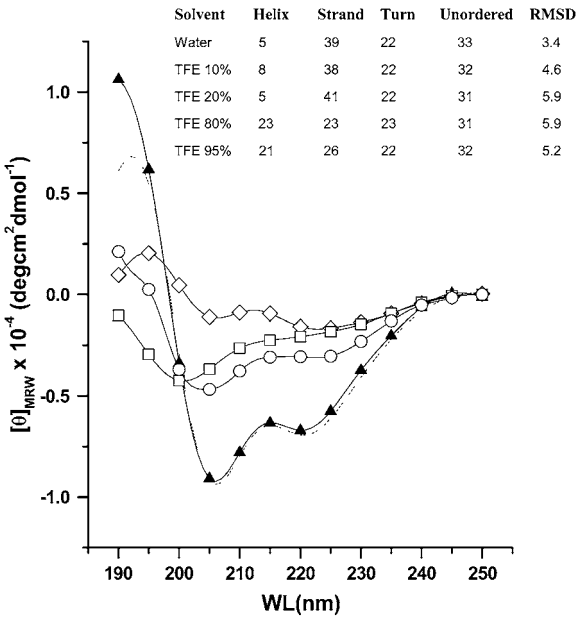

FIGURE 10 CD spectra of EX1–7, 10 μM in water (□), 10% TFE (○), 20% TFE (◇), 80% TFE (_), and 95% TFE (▲). The inset shows the fractions of secondary structure estimated from the deconvoluted CD spectra by the Contin method.

Supplementary Material). By analogy with tropoelastin (15) the polypeptide undergoes an inverse-temperature aggregation whose critical temperature (T_c) is dependent on the ionic strength of the medium. As a matter of fact, T_c is shifted to lower temperature in PBS where the peptide exhibits a value of ~37°C surprisingly identical to that shown by human tropoelastin under similar conditions. However, differently

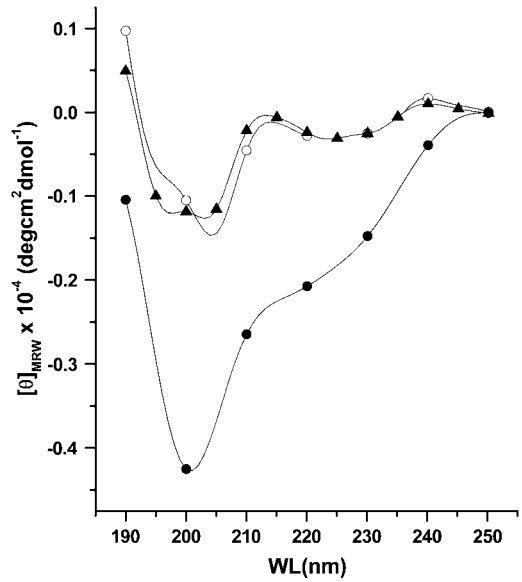

FIGURE 11 CD spectra of EX1–7, 10 μM in water at 20°C (●), 30°C (○), and 40°C (▲).

from the entire protein, the process is not reversible and, therefore, does not appear to be an authentic coacervation but rather an irreversible aggregation. This looks like what was previously coded for the peptide sequence by exon 30 of human tropoelastin and demonstrated originate from the deposition of amyloid fibers (23). To confirm the formation of amyloid fibers, a typical Congo red dye binding assay was performed. EX1–7 aggregates not only bind the dye, but also showed green-yellow birefringence in polarized light as usually found for the highly ordered, cross-β-sheet structure typical of amyloids (see Supplementary Material). The supramolecular structures were studied by TEM (Fig. 12). Here, the emerging picture is rather complex: EX1–7 is, in fact, able to display all the supramolecular organizations of elastin, so demonstrating to be an authentic model for the entire protein. After heating, the aqueous solution of the polypeptide gave rise to globular structures with diameters ranging from 7 to 35 nm (Fig. 12 *A*) and fibrils with diameter of 7 nm (Fig. 12 *B*). In PBS, twisted fibers appear with a diameter of either 30–37 nm (Fig. 12 *C*) or 55–73 nm (Fig. 12 *D*) and a length of 1 μm. Besides these structures, we also found a few elastinlike fibers (Fig. 12, *E* and *F*). Although amyloidlike fibers were previously found in one elastin sequence (EX 30), the predominance of these fibers in EX1–7 was unexpected, taking in mind that this exon is expected to be highly representative of entire elastin.

To investigate the role of the signal peptide, we have studied the structure and the ultrastructure of MAGL-TAAAPRPGVLLLLLSILHPSRPG (EX1). The CD spectra at different TFE concentrations are reported in Fig. 13. EX1 shows a random conformation plus PPII structure in water according to a qualitative evaluation of the spectra. In less polar media, such as 10% TFE, a curve typical of the β-structure was observed whereas a predominant α-helical conformation was observed at higher TFE percentages. Turbidimetry measurements did not show significant coacervation phenomena (data not shown). TEM showed twisted fibers of 8-nm diameter and globules of 20–40 nm on the sample in PBS heated at 60°C for four days (Fig. 14 *A*) and several amyloids (33) with an average diameter of 20 nm in the aqueous solution (Fig. 14 *B*). A fibrillar network and a few fibrils of 3–4 nm diameter are observed if the peptide is left in 16X-PBS for two days at room temperature (Fig. 14 *C*).

DISCUSSION

According to the documented fractal properties of elastin (28,34,35), which means that the protein is characterized by the property of statistical self-similarity, even very short sequences show molecular and supramolecular features very similar to those of the entire protein (28,35,36). This finding is most likely related to the abundance of repeating sequences of elastin, the repetition being found at different scales along the whole sequence of the molecule (37). This allows the system to be studied by analyzing its constituents one by one, in an

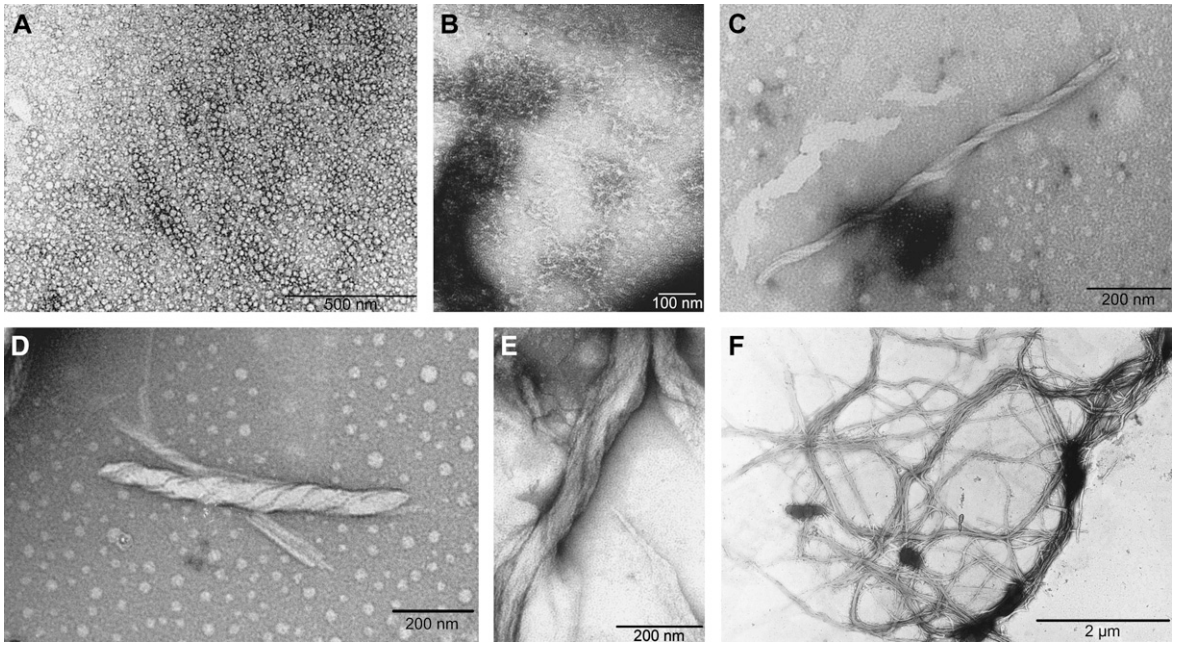

FIGURE 12 TEM micrographs of EX1–7, 250 μM, and at 60°C: (*A* and *B*) in water for one day; (*C* and *D*) in PBS for 4 days; and (*E* and *F*) in PBS, for one and for six days, respectively.

attempt to overcome the experimental difficulties connected with the study of a big, highly insoluble, molecule, such as elastin.

The main results obtained by CD spectroscopy on the decapeptide and octadecapeptide at different temperatures and ionic strengths show a conformational transition from PPII to β-sheet and/or to type I β-turn. The PPII structure is mainly favored in water at low temperatures as expected for a conformation devoid of intramolecular hydrogen bonds, such as those present in α-helices and β-turns, and stabilized by hydrogen bonding with solvent molecules (3,38). This finding explains the ''flexibility'' of PPII conformation that can easily convert to other conformations on changing the microenvironment conditions such as temperature and ionic strength (39). Furthermore, it is to be noted that the PPII conformation has been observed in another elastomeric protein, titin (40). This protein is composed of two domains, one of them consisting of tandem repeats of a fundamental module that averages 28 residues, mostly of PEVK residues. A PEVK fragment containing 16 PEVK modules of 469 residues was studied by CD and revealed the presence of PPII structure with flexible joints. Therefore, PPII conformation is widely found also in small peptides and not only in larger ones (41–44). In fact, the CD spectra carried out under physiological conditions, shown in Fig. 2, *B* and *C*, indicate that a significant population of PPII structure is present in the octadecapeptide. The supramolecular organization observed for the octadecapeptide, which coacervates, was found to be very similar to that already found for the coacervates of tropoelastin and α-elastin (13). In fact, the fibers observed are characterized by an arrangement of parallel filaments along the length of the fiber. Studies carried out on single exons have shown that the propensity of the elastin sequences to be structured in apolar solvents is a common peculiarity for these sequences even if the relative amounts of α, β, and PPII structures and random coil depend on the particular sequence (37).

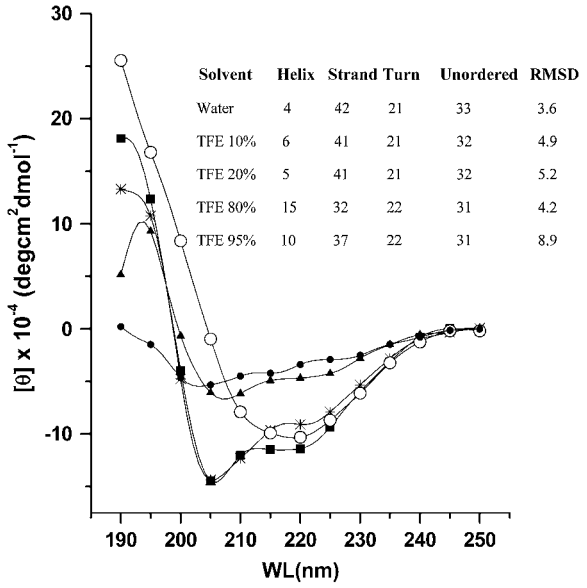

FIGURE 13 CD spectra of EX1, 37 μM in water (●), 10% TFE (○), 20% TFE (▲), 80% TFE (*), and 95% TFE (■). In this case, where the contribution of PPII structure is presumably relevant, the Contin method gave non-auto-coherent results, and therefore is not reported.

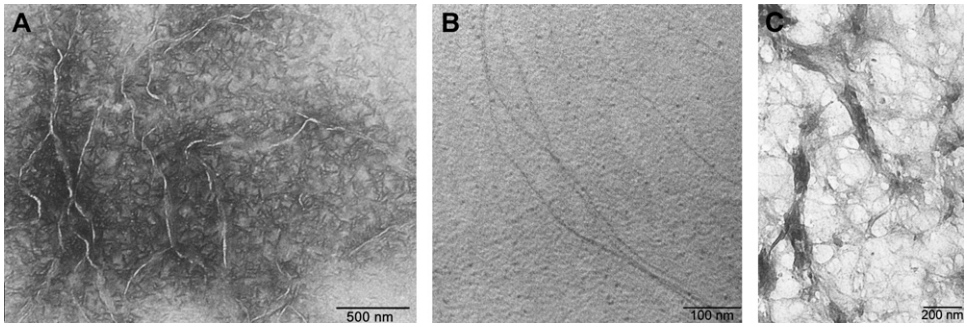

FIGURE 14 TEM micrographs of EX1 (*A*) 100 μM in PBS for four days; (*B*) 400 μM in water at 60°C for four days; and (*C*) 176 μM in 16X-PBS for one day at room temperature.

The N-terminal region of human tropoelastin, in which all the main structural motifs of the whole protein are present such as the glycine-rich hydrophobic regions (encoded by exons 2, 3, and 7) and the moieties representing the cross-linking domains, both of KP and KA type (encoded by exons 4 and 6, respectively), exhibits a structural organization similar to that found for the other regions of elastin. In fact, the CD spectrum of EX2–7 also essentially shows a random coil conformation in water and α-helix, β-strand, and β-turn structures in equilibrium between them in TFE/water mixture. As a general rule, TFE favors folded conformations inducing periodic and/or rigid structures (not only α-helices as commonly thought). The rationale for that may be found in Roccatano et al. (45) and Tamburro et al. (37). Obviously, the problem arises as to whether TFE may be considered a relevant environment as compared to the physiological conditions. As a matter of fact, nobody knows the dielectric constant of the physiological microenvironment; however, a reasonable assumption is that it has an intermediate value between the highly polar aqueous solvent and TFE. In this sense, the results obtained for exon-coded polypeptide sequences of human tropoelastin (37,46) strongly suggested that the probable ''physiological'' structures are actually accounted for by equilibria between the different conformer populations found in water and TFE, respectively. Moreover, EX2–7 coacervates at 37°C like the entire tropoelastin and indeed electron microscopy, atomic force microscopy, and optical microscopy show the presence of elastinlike fibers as well as small amounts of amyloid fibers (see Figs. 7–9). It is of paramount importance that those structures (and the other ones found) are independent of the scale of the observation and of the presence of water because they were observed for both dehydrated (by TEM) and hydrated (by AFM and optical microscopy) samples. EX1–7, which includes the signal peptide, does not coacervate, but gives an irreversible precipitate. TEM shows variously sized amyloid fibers under different experimental conditions. In this case, amyloid fibers are dominant and are of considerable size in salt solution, whereas in water many globules are also present. The different properties observed for EX1–7 and EX2–7 may suggest the reason for which the signal peptide must be removed. As reported by Saunders et al. (47), the signal peptide of elastin is removed in the lumen of the endoplasmic reticulum before the protein is fully synthesized. Our results indicate that the cleavage of the signal peptide strongly reduces the amyloidlike fiber formation and allows the protein to adopt the correct folding to perform its function. In fact, EX2–7, differently from EX1–7, is able to coacervate. Since the coacervation is considered the first event for the correct assembly of the elastic fibers, the removal of the signal peptide is an essential event to obtain a functional tropoelastin.

A summary of the obtained results is reported in Table 2. We note that the β-structure is ubiquitous in all the sequences studied except for the decapeptide where PPII and type II β-turn dominate. Accordingly, the presence of a β-structure is a necessary, although not sufficient, requirement for the appearance of amyloid fibers. The results of this article, together with those already published on exon 30 of human tropoelastin (23), confirm that there is no need for particular sequences to get amyloid fiber deposition as previously stated by Stefani and Dobson (48). Rather, it is the length of particular sequences that appears to be important: in the case of elastin sequences, in contrast to other proteins (see, for example, the Alzheimer amyloids) in which

TABLE 2 Summary of the molecular and supramolecular elastin polypeptide structures

Peptide	Molecular structure	Supramolecular structure
Octadecapeptide	β-structure (H_2O).	Elastinlike organization.
Decapeptide	PPII + type II β-turn (H_2O).	Elastinlike organization.
EX2–7	β-strand + turns + unordered (H_2O). Increase of α-helix (TFE).	Globular, unbranched amyloidlike fibrils and ribbonlike fibers.
EX1–7	β-strand + turns + unordered (H_2O). Increase of α-helix (TFE).	Fibrillar, elastinlike organization and amyloid fibers.
EX1	Essentially random coil + PPII (H_2O). Small increase of α-helix (TFE).	Twisted-fibers, amyloid fibrils, fibrillar network.

even 5–7 residues are sufficient, a minimal length of ~20 amino-acid residues seems to be necessary.

Our results on the elastin representative peptides, EX1–7 and EX2–7, suggest that formation of amyloid fibers, under proper conditions, could be promoted not only by specific mutations (49) and fragment removal (50–52) but also by the presence of additional sequences such as the signal sequence, which may confer particular structural features to an otherwise unstable precursor that can evolve to a cross-β structure and then to amyloid formation. These arguments are in agreement with previous experimental results in which insufficient processing of human pro-islet amyloid polypeptide results in increased amyloid formation (53).

Another point is that, as is known, the primary transcript of tropoelastin undergoes extensive alternative splicing, resulting in the translation of multiple heterogeneous protein isoforms (54). Our results on the sequences contained in the EX30 show that they give amyloid or elastinlike fibers depending on their length and neighboring sequences. Therefore, we suggest that the multiple elastin isoforms may have different propensities to give rise to fibers with different features as recently has been demonstrated in other proteins (55).

SUPPLEMENTARY MATERIAL

To view all of the supplemental files associated with this article, visit www.biophysj.org.

This work was supported by the European Community Project ''ELASTAGE'' grant No. 018960.

Thanks are due to Mr. Alessandro Laurita (CIM, Interdepartmental Centre of Microscopy, University of Basilicata) for the TEM micrographs and the optical microscopy images in polarized light and to Dr. Angelo De Stradis for the TEM micrographs. Special thanks are also due to Dr. Loretta del Mercato (Istituto Superiore Universitario di Formazione-Centro Nazionale delle Ricerche, Lecce) for AFM images of the octadecapeptide and for AFM images of the EX2–7 to Dr. Roberta Flamia who made also optical microscopy images.

REFERENCES

1. Gibson, M. A., G. Hatzinikolas, J. S. Kumaratilake, L. B. Sandberg, J. K. Nicholl, G. R. Sutherland, and E. G. Cleary. 1996. Further characterization of proteins associated with elastic fiber microfibrils including the molecular cloning of MAGP-2 (MP25). *J. Biol. Chem.* 271:1096–1103.
2. Debelle, L., and A. M. Tamburro. 1999. Elastin: molecular description and function. *Int. J. Biochem. Cell Biol.* 31:261–272.
3. Bochicchio, B., N. Floquet, A. Pepe, A. J. P. Alix, and A. M. Tamburro. 2004. Dissection of human tropoelastin: solution structure, dynamics and self-assembly of the exon 5 peptide. *Chemistry A Eur. J.* 10:3166–3176.
4. Urry, D. W., and M. M. Long. 1977. On the conformation, coacervation and function of polymeric models of elastin. *Adv. Exp. Med. Biol.* 79:685–714.
5. Urry, D. W., D. C. Gowda, T. M. Parker, C. H. Luan, M. C. Reid, C. M. Harris, A. Pattanaik, and R. D. Harris. 1992. Hydrophobicity of amino acid residues: differential scanning calorimetry and synthesis of the aromatic analogues of the polypentapeptide of elastin. *Biopolymers.* 32:1243–1250.
6. Miao, M., C. M. Bellingham, R. J. Stahl, E. E. Sitarz, C. J. Lane, and F. W. Keeley. 2003. Sequence and structure determinants for the self-aggregation of recombinant polypeptides modeled after human elastin. *J. Biol. Chem.* 278:48553–48562.
7. Partridge, S., H. Davis, and G. Adair. 1955. The chemistry of connective tissues. 2. Soluble proteins derived from partial hydrolysis of elastin. *Biochem. J.* 61:11–21.
8. Urry, D. W., B. Starcher, and S. M. Partridge. 1969. Coacervation of solubilized elastin effects a notable conformational change. *Nature.* 222: 795–796.
9. Jamieson, A., C. Downs, and A. Walton. 1972. Studies of elastin coacervation by quasielastic light scattering. *Biochim. Biophys. Acta.* 271:34–47.
10. Podrazky, V., and D. Jackson. 1976. Collection Czechoslov. *Chem. Commun.* 41:2296–2302.
11. Castiglione-Morelli, M. A., M. DeBiasi, A. DeStradis, and A. M. Tamburro. 1993. An aggregating elastinlike pentapeptide. *J. Biomol. Struct. Dyn.* 11:181–190.
12. Reiersen, H., A. Clarke, and A. Rees. 1998. Short elastinlike peptides exhibit the same temperature-induced structural transitions as elastin polymers: implications for protein engineering. *J. Mol. Biol.* 283:255–264.
13. Cox, B., B. Starcher, and D. Urry. 1974. Communication: Coacervation of tropoelastin results in fiber formation. *J. Biol. Chem.* 249:997–998.
14. Bressan, G., I. Pasquali-Ronchetti, C. Fornieri, F. Mattioli, I. Castellani, and D. Volpin. 1986. Relevance of aggregation properties of tropoelastin to the assembly and structure of elastic fibers. *J. Ultrastruct. Res.* 94:209–216.
15. Vrhovski, B., S. Jensen, and A. Weiss. 1997. Coacervation characteristics of recombinant human tropoelastin. *Eur. J. Biochem.* 250:92–98.
16. Bellingham, C. M., K. A. Woodhouse, P. Robson, S. J. Rothstein, and F. W. Keeley. 2001. Self-aggregation characteristics of recombinantly expressed human elastin polypeptides. *Biochim. Biophys. Acta.* 1550:6–19.
17. Cox, B. A., B. C. Starcher, and D. W. Urry. 1973. Coacervation of α-elastin results in fiber formation. *Biochim. Biophys. Acta.* 317:209–213.
18. Urry, D. W., M. M. Long, B. A. Cox, T. Ohnishi, L. W. Mitchell, and M. Jacobs. 1974. The synthetic polypentapeptide of elastin coacervates and forms filamentous aggregates. *Biochim. Biophys. Acta.* 371:597–602.
19. Bellingham, C. M., M. A. Lillie, J. M. Gosline, G. M. Wright, B. Starcher, A. J. Bailey, K. A. Woodhouse, and F. W. Keeley. 2003. Recombinant human elastin polypeptides self-assemble into biomaterials with elastinlike properties. *Biopolymers.* 70:445–455.
20. Keeley, F. W., C. M. Bellingham, and K. A. Woodhouse. 2002. Elastin as a self-organizing biomaterial: use of recombinantly expressed human elastin polypeptides as a model for investigations of structure and self-assembly of elastic. *Philos. Trans. R. Soc. Lond. B Biol. Sci.* 357:185–189.
21. Pepe, A., D. Guerra, B. Bochicchio, D. Quaglino, D. Gheduzzi, I. Pasquali-Ronchetti, and A. M. Tamburo. 2005. Dissection of human tropoelastin: supramolecular organization of polypeptide sequences coded by particular exons. *Matrix Biol.* 24:96–109.
22. Clarke, A. W., E. C. Arnspang, S. M. Mithieux, E. Korkmaz, F. Braet, and A. S. Weiss. 2006. Tropoelastin massively associates during coacervation to form quantized protein spheres. *Biochemistry.* 45:9989–9996.
23. Tamburro, A. M., A. Pepe, B. Bochicchio, D. Quaglino, and I. Pasquali-Ronchetti. 2005. Supramolecular amyloidlike assembly of the polypeptide sequence coded by exon 30 of human tropoelastin. *J. Biol. Chem.* 280:2682–2690.
24. King, D. S., C. G. Fields, and G. B. Fields. 1990. A cleavage method which minimizes side reactions following Fmoc solid phase peptide synthesis. *Int. J. Pept. Protein Res.* 36:255–266.
25. Perczel, A., M. Hollosi, P. Sandor, and G. D. Fasman. 1993. The evaluation of type I and type II β-turn mixtures. Circular dichroism, NMR and molecular dynamics studies. *Int. J. Pept. Protein Res.* 41:223–236.

26. Gotte, L., M. G. Giro, D. Volpin, and R. W. Horne. 1974. The ultrastructural organization of elastin. *J. Ultrastruct. Res.* 46:23–33.
27. Volpin, D., D. W. Urry, B. A. Cox, and L. Gotte. 1976. Optical diffraction of tropoelastin and α-elastin coacervates. *Biochim. Biophys. Acta.* 439:353–358.
28. Tamburro, A. M., A. De Stradis, and L. D'Alessio. 1995. Fractal aspects of elastin supramolecular organization. *J. Biomol. Struct. Dyn.* 12:1161–1172.
29. Srisailam, S., H. M. Wang, T. K. S. Kumar, D. Rajalingam, V. Sivaraja, H. S. Sheu, Y. C. Chang, and C. Yu. 2002. Amyloidlike fibril formation in an all β-barrel protein involves the formation of partially structured intermediate(s). *J. Biol. Chem.* 277:19027–19036.
30. Tamburro, A. M., V. Guantieri, D. Daga-Gordini, and G. Abatangelo. 1977. Conformational transitions of α-elastin. *Biochim. Biophys. Acta.* 492:370–376.
31. Debelle, L., A. J. Alix, M. P. Jacob, J. P. Huvenne, M. Berjot, B. Sombret, and P. Legrand. 1995. Bovine elastin and κ-elastin secondary structure determination by optical spectroscopies. *J. Biol. Chem.* 270: 26099–26103.
32. Martino, M., A. Bavoso, V. Guantieri, A. Coviello, and A. M. Tamburo. 2000. On the occurrence of polyproline II structure in elastin. *J. Mol. Struct.* 519:173–189.
33. Zandomeneghi, G., M. R. H. Krebs, M. G. McCammon, and M. Fandrich. 2004. FTIR reveals structural differences between native β-sheet proteins and amyloid fibrils. *Protein Sci.* 13:3314–3321.
34. Tamburro, A. M., D. Daga-Gordini, V. Guantieri, and A. De Stradis. 1994. On the molecular and the supramolecular structure of elastin. *In* Chemistry and Properties of Biomolecular Systems, Vol. 2. N. Russo, S. Anastassopoulou, and G. Barone, editors. Kluwer, Dordrecht.
35. D'Alessio, L., A. M. Tamburro, and A. De Stradis. 1999. Observation of fractal structures in the supramolecular organization of protein molecules. INRIA, Delft, June 14–16. *Proc. Fractals Eng.*
36. Tamburro, A. M. 1995. The supramolecular structures of elastin and related synthetic polypeptides: Scale invariant weaving. *In* Macrocyclic and Supramolecular Chemistry in Italy. G. Savelli, editor. Centro Stampa Università di Perugia, Italy.
37. Tamburro, A. M., B. Bochicchio, and A. Pepe. 2003. Dissection of human tropoelastin: exon-by-exon chemical synthesis and related conformational studies. *Biochemistry.* 42:13347–13362.
38. Bochicchio, B., and A. M. Tamburro. 2002. Polyproline II structure in proteins: identification by chiroptical spectroscopies, stability, and functions. *Chirality.* 14:782–792.
39. Tamburro, A. M., B. Bochicchio, and A. Pepe. 2005. The dissection of human tropoelastin: from the molecular structure to the self-assembly to the elasticity mechanism. *Pathol. Biol.* 53:383–389.
40. Ma, K., and K. Wang. 2003. Malleable conformation of the elastic PEVK segment of titin: non-co-operative interconversion of polyproline II helix, β-turn and unordered structures. *Biochem. J.* 374: 687–695.
41. Ma, K., L. Kan, and K. Wang. 2001. Polyproline II helix is a key structural motif of the elastic PEVK segment of titin. *Biochemistry.* 40:3427–3438.
42. Gutierrez-Cruz, G., A. H. Van Heerden, and K. Wang. 2001. Modular motif, structural folds and affinity profiles of the PEVK segment of human fetal skeletal muscle titin. *J. Biol. Chem.* 276:7442–7449.
43. Shi, Z., K. Chen, Z. Liu, T. R. Sosnick, and N. R. Kallenbach. 2006. PII structure in the model peptides for unfolded proteins: studies on ubiquitin fragments and several alanine-rich peptides containing QQQ, SSS, FFF, and VVV. *Proteins.* 63:312–321.
44. Zerella, R., P. A. Evans, J. M. Ionides, L. C. Packman, B. W. Trotter, J. P. Mackay, and D. H. Williams. 1999. Autonomous folding of a peptide corresponding to the N-terminal β-hairpin from ubiquitin. *Protein Sci.* 8:1320–1331.
45. Roccatano, D., G. Colombo, M. Fioroni, and A. E. Mark. 2002. Mechanism by which 2,2,2-trifluoroethanol/water mixtures stabilize secondary-structure formation in peptides: a molecular dynamics study. *Proc. Natl. Acad. Sci. USA.* 99:12179–12184.
46. Tamburro, A. M., A. Pepe, and B. Bochicchio. 2006. Localizing α-helices in human tropoelastin: assembly of the elastin ''puzzle''. *Biochemistry.* 45:9518–9530.
47. Saunders, N. A., and M. E. Grant. 1984. Elastin biosynthesis in chick-embryo arteries. Studies on the intracellular site of synthesis of tropoelastin. *Biochem. J.* 221:393–400.
48. Stefani, M., and C. M. Dobson. 2003. Protein aggregation and aggregate toxicity: new insights into protein folding, misfolding diseases and biological evolution. *J. Mol. Med.* 81:678–699.
49. Concepcion, G. P., and E. A. Padlan. 2005. Why don't humans get scrapie from eating sheep? A possible explanation based on secondary structure predictions. *Med. Hypotheses.* 65:865–867.
50. Kelly, J. W. 1998. The alternative conformations of amyloidogenic proteins and their multi-step assembly pathways. *Curr. Opin. Struct. Biol.* 8:101–106.
51. Lansbury, P. T. 1999. Evolution of amyloid: what normal protein folding may tell us about fibrillogenesis and disease. *Proc. Natl. Acad. Sci. USA.* 96:3342–3344.
52. Perutz, M. F. 1999. Glutamine repeats and neurodegenerative diseases: molecular aspects. *Trends Biochem. Sci.* 24:58–63.
53. Paulsson, J. F., and G. T. Westermark. 2005. Aberrant processing of human pro-islet amyloid polypeptide results in increased amyloid formation. *Diabetes.* 54:2117–2125.
54. Sato, F., H. Wachi, B. C. Starcher, H. Murata, S. Amano, S. Tajima, and Y. Seyama. 2006. The characteristics of elastic fiber assembled with recombinant tropoelastin isoform. *Clin. Biochem.* 39:746–753.
55. Holtzman, D. M., K. R. Bales, T. Tenkova, A. M. Fagan, M. Parsadanian, L. J. Sartorius, B. Mackey, J. Olney, D. McKeel, D. Wozniak, and S. M. Paul. 2000. Apolipoprotein E isoform-dependent amyloid deposition and neuritic degeneration in a mouse model of Alzheimer's disease. *Proc. Natl. Acad. Sci. USA.* 97:2892–2897.